

Integrated Adaptive Feed-forward Control of Atmospheric Turbulence excited Rigid Body Motions and Structural Vibrations on a Large Transport Aircraft

Andreas Wildschek, and Rudolf Maier

Abstract—An adaptive feed-forward controller for simultaneous compensation of atmospheric turbulence excited rigid body motions and structural vibrations is designed. Proposed feed-forward control is intended as an add-on to current gust load alleviation systems. The objectives thereby are increased passenger comfort and handling qualities, as well as a more efficient reduction of dynamic wing loads. A steepest descent algorithm is applied in order to increase the robustness of the performance of the feed-forward control system against modeling errors and variations of wing tanks configuration and Mach number. The proposed algorithm is tested in numeric simulations with the state space model of a conventional four-engine transport aircraft. The simulation results illustrate the proposed control system's high potential for simultaneous compensation of atmospheric turbulence excited pitch and wing bending accelerations.

Index Terms— Multi-objective control, gust load alleviation, adaptive feed-forward control, atmospheric disturbance compensation, control of flexible aircraft.

I. INTRODUCTION

TODAY large transport aircraft are commonly equipped with gust load alleviation systems. The objective of these control systems is the reduction of atmospheric turbulence excited static and dynamic loads, as well as an increase of passenger comfort and handling qualities. In [1] the design of a robust feedback system for wing bending control is proposed.

The aeroelastic plant however varies with wing tanks configuration and Mach number. The thereby imposed robust stability constraints limit the obtainable control performance. Therefore, in [2] a gain scheduled feedback control architecture is proposed for the reduction of maneuver and gust loads over a wide flight envelope.

Since feed-forward control is expected to improve the obtainable control performance, a nose boom alpha vane signal for the compensation of static gust loads is used in [3]. In a recent paper [4] it was shown that an alpha probe can provide a proper reference signal for the feed-forward compensation of dynamic gust loads too. For a maximum alleviation of wing bending vibrations a hybrid SISO (Single Input Single Output) controller (i.e. combined robust

feedback/adaptive feed-forward control using symmetrically driven ailerons as actuators) has been proposed in [4].

However, herein the compensation of atmospheric turbulence (i.e. continuous gust) excited rigid body motions was not considered. The adaptation of the feed-forward path increases its robustness against deviations of the plant phase and magnitude from the nominal design point value without any performance loss as shown in [5]. Note, that feed-forward control is generally more performance sensitive to phase and magnitude errors than feedback control.

In this paper an adaptive MIMO (Multiple Input Multiple Output) feed-forward controller is designed for a conventional large transport aircraft. Thereby the objective is a simultaneous compensation of atmospheric turbulence (i.e. continuous gust) excited rigid body motions and structural vibrations using all available control surfaces of sufficient bandwidth (e.g. elevator, ailerons, rudder, additional trailing edge devices, etc.).

II. DESIGN OF ADAPTIVE MIMO FEED-FORWARD CONTROL

A. The Adaptive Control Algorithm

The objective of the proposed adaptive MIMO control algorithm is the minimization of the quadratic H_2 norm of the L error signals e_l , i.e. the minimization of the cost function J :

$$J = \langle \bar{e}^T \bar{e} \rangle \quad (1)$$

with:

$$\bar{e} = [e_1, e_2, \dots, e_l, \dots, e_L]^T \quad (2)$$

The superscript \top is the transpose, and the brackets $\langle \dots \rangle$ denote the expectation value. For the derivation of the adaptive feed-forward control algorithm all reference signals are assumed to be:

- I. Persistently exciting (i.e. the adaptive controller can be turned on only when a predefined threshold of turbulence strength is exceeded), and
- II. Ergodic (i.e. the ensemble average may be replaced by the time average).

Manuscript received September 18, 2007.

Andreas Wildschek and Rudolf Maier are with EADS Innovation Works Germany, 81663 Munich; Phone: +49-89-607-27189; Fax: +49-89-607-23067; E-mail: Andreas.Wildschek@EADS.net, Rudolf.Maier@EADS.net

III. The parasitic feedback from the actuators to the reference signals is small enough to be neglected.

IV. It is also assumed that all reference signals have enough lead time to allow causality of the optimum controller. In [6] it was recently shown that a sensor fusion between alpha probe and LIDAR can increase the reference lead-time while maintaining the accuracy of the alpha probe. So assumption IV. is definitely accomplishable.

As reference sensors alpha and beta probes, differential pressure sensors at the front fuselage and leading edges, as well as LIDAR are thinkable. Let k be the number of the reference signal with K available references. Then, at time step n , the discrete-time MIMO feed-forward control law for the m^{th} actuator u_m is:

$$u_m(n) = \sum_{k=1}^K \bar{h}_{mk}(n)^T \cdot \bar{\alpha}_k(n) = \sum_{k=1}^K \bar{\alpha}_k^T(n) \cdot \bar{h}_{mk}(n) \quad (3)$$

with mk^{th} FIR (Finite Impulse Response) control filter:

$$\bar{h}_{mk}(n) = [h_{0_{mk}}(n), h_{1_{mk}}(n), \dots, h_{N-1_{mk}}(n)]^T \quad (4)$$

Thereby, $h_{0_{mk}}(n), h_{1_{mk}}(n), \dots, h_{N-1_{mk}}(n)$ are the coefficients of the mk^{th} FIR control filter, and N denotes the control filter length, which is assumed to be equal for all mk controllers for the sake of straightforwardness of notation. $\bar{\alpha}_k(n)$ is the vector of the sampled k^{th} reference signal at time step n :

$$\bar{\alpha}_k(n) = [\alpha_k(n), \alpha_k(n-1), \dots, \alpha_k(n-N+1)]^T \quad (5)$$

The frequency domain steepest descent update law for the mk^{th} FIR control filter is taken similar to the one proposed in [7]:

$$\bar{h}_{mk}(n) = \bar{h}_{mk}(n-1) - IDFT \left\{ \sum_{l=1}^L \frac{c_{lmk}}{L} \cdot (\hat{R}_{lmk}^*(n, f) E_l(n, f)) \right\}_+ \quad (6)$$

Thereby, $IDFT\{\dots\}_+$ denotes the causal share of the Inverse Discrete Fourier Transform of the quantity inside $\{\dots\}$ with f denoting the discrete frequency. The superscript $*$ denotes complex conjugation and c_{lmk} is the lmk^{th} convergence coefficient. Then $\hat{R}_{lmk}(n, f)$ is the Discrete Fourier Transform (DFT) of the latest $2N$ -point segment of the sampled *estimated* filtered reference signal \hat{r}_{lmk} , which is the sampled reference signal $\bar{\alpha}_k$ filtered by

the transfer path \hat{G}_{lm} . Thereby, \hat{G}_{lm} is an estimate of the plant's transfer path from the m^{th} control command u_m to the l^{th} error signal e_l , which is denoted G_{lm} . Furthermore, $E_l(n, f)$ is the $2N$ -point DFT of the latest N point segment of e_l padded with N zeros. Finally, only the causal share of the quantity inside the brackets $\{\dots\}$ is used. This approach is called *overlap-save method* [8], and prevents circular correlation.

Provided that with angular frequency ω and sample period T :

V. the optimum MIMO feed-forward controller is causal, and

VI. both, $\mathbf{G}(e^{j\omega T})^H \mathbf{G}(e^{j\omega T})$, and

VII. $\mathbf{S}_{\alpha\alpha}(e^{j\omega T})$ are non-singular,

the cost function J has a unique global minimum [9].

Thereby, $\mathbf{G}(e^{j\omega T})$ is the $L \times M$ matrix of the plant's frequency responses $G_{lm}(e^{j\omega T})$ and the superscript H denotes the Hermitian transpose. According to assumption VI no optimum controller exists for frequencies where the magnitude of a plant transfer function is zero (i.e. non-controllability.) The positive definiteness of the spectral density matrix of the K reference signals

$$\mathbf{S}_{\alpha\alpha}(e^{j\omega T}) = \langle \bar{A}(e^{j\omega T}) \bar{A}(e^{j\omega T})^H \rangle \quad (7)$$

is ensured by the assumption of persistent excitation (i.e. assumption I.) Thereby, $\bar{A}(e^{j\omega T})$ is the vector of the Fourier transforms $A_k(e^{j\omega T})$ of the K sampled reference signals.

Then the optimum frequency domain controller can be written as [9]:

$$\mathbf{H}_{opt}(e^{j\omega T}) = -[\mathbf{G}(e^{j\omega T})^H \mathbf{G}(e^{j\omega T})]^{-1} \mathbf{G}(e^{j\omega T})^H \mathbf{S}_{\alpha\alpha}^{-1} \quad (8)$$

Thereby, $\mathbf{S}_{\alpha\alpha}$ is the $L \times K$ cross spectral density matrix between the K reference signals and the L disturbance signals d_l , i.e. the L error signals when the MIMO feed-forward controller is turned off, compare [9]:

$$\mathbf{S}_{\alpha\alpha}(e^{j\omega T}) = \langle \bar{D}(e^{j\omega T}) \bar{A}(e^{j\omega T})^H \rangle \quad (9)$$

Thereby $\bar{D}(e^{j\omega T})$ is the vector of the Fourier transforms $D_l(e^{j\omega T})$ of the L sampled disturbance signals d_l .

B. Stability of the Controller Adaptation

Stable convergence of the update law (6) is achieved by the choice of the convergence coefficients c_{lmk} . If the c_{lmk} are too small the algorithm converges very slowly which would not be useful since flight phases encountering rough atmospheric vibration excitation are generally of limited duration. If the c_{lmk} are chosen to high, the adaptation becomes unstable.

In a previous paper this robust stability problem has been solved for the SISO case [5]. Applying these results to the MIMO case, the following boundaries for stable convergence of the controllers \bar{h}_{mk} are suggested:

$$0 < c_{lmk} < \left[\frac{2 \cdot F_{error_{lm}}(f)}{(2 \cdot \Delta_{lm} + 1) \cdot \tilde{S}_{\hat{r}_{lmk}}(n, f)} \right]_{\text{Minimum over } f} \quad (10)$$

The stability bounds in (10) still need to be proven. $\tilde{S}_{\hat{r}_{lmk}}(f)$ denotes the *instantaneous estimate* of the power spectral density of the estimated filtered reference signal \hat{r}_{lmk} :

$$\tilde{S}_{\hat{r}_{lmk}}(n, f) = \left\{ \hat{R}_{lmk}(n, f) \hat{R}_{lmk}^H(n, f) \right\}_+ \quad (11)$$

The function $F_{error_{lm}}(f)$ describes the magnitude and phase error in the plant estimates $\hat{G}_{lm}(f)$:

$$F_{error_{lm}}(f) = \frac{|\hat{G}_{lm}(f)|}{|G_{lm}(f)|} \cdot \cos(\phi_{G_{lm}}(f) - \phi_{\hat{G}_{lm}}(f)) \quad (12)$$

Thereby, $\phi_{G_{lm}}(f)$ and $\phi_{\hat{G}_{lm}}(f)$ denote the phase angles of the evaluation of the $2N$ -point DFT of the real plant's impulse response $G_{lm}(f)$ and of its estimate $\hat{G}_{lm}(f)$ at the discrete frequency f , and $|G_{lm}(f)|$ and $|\hat{G}_{lm}(f)|$ are the correspondent magnitudes. From (12) one can see, that the convergence coefficient can be adjusted so that the adaptation, and thus the control performance of the converged MIMO feed-forward controller is robust against uncertainties in the plant model.

The key issue about $\tilde{S}_{\hat{r}_{lmk}}(n, f)$ denoting an *instantaneous estimate* of the power spectral density of the estimated filtered reference signal is that $\tilde{S}_{\hat{r}_{lmk}}(n, f)$ can be calculated at each time step n anew which allows for continuous online calculation of the upper boundaries of the convergence coefficients c_{lmk} . The term Δ_{lm} denotes the *maximum feedback delay* of the lm^{th} plant transfer function $G_{lm}(e^{j\omega T})$:

$$\Delta_{lm} = \Delta_{\text{overlap}} - 1 + \Delta_{G_{lm}} \quad (13)$$

This *maximum feedback delay* is due to two effects:

- Firstly, the plant (including the digital feed-forward controller, digital to analogue, and analogue to digital converter, as well as anti-aliasing filters) introduces a (frequency dependent) group delay $-\partial\phi_{G_{lm}}(\omega)/\partial\omega$ between the m^{th} sampled-time control command $u_m(n)$ and the l^{th} sampled-time error signal $e_l(n)$. The *maximum* of this group delay in the controlled frequency range is *rounded down* to an integer value. This integer value corresponds to a delay of $\Delta_{G_{lm}}$ samples.
- Secondly, although the controller is updated every time step n for smooth convergence of its coefficients, the quantity inside $IDFT\{\dots\}_+$ is generally updated only every $\Delta_{\text{overlap}}^{\text{th}}$ sample for a reduction of required computing power (i.e. usually very important on a flight computer). Thus, the update of the quantity inside $IDFT\{\dots\}_+$ is additionally delayed by $\Delta_{\text{overlap}}-1$ samples in the worst case.

III. NUMERIC SIMULATIONS

The proposed adaptive MIMO feed-forward control algorithm was tested numerically on a state space model of the longitudinal aeroelastic dynamics of a large conventional four-engine transport aircraft for various wing tanks configurations and Mach numbers. An alpha probe mounted at the front fuselage is used as reference sensor (i.e. $K=1$.) For convenience it is thereby assumed in this paper that the reference signal is perfectly correlated with the disturbance of the aircraft. The atmospheric excitation is modeled by filtered white noise representing a von Kármán turbulence spectrum with a scale of turbulence of 762 meters.

Note that an alpha probe generally does not provide such a perfectly correlated reference signal leading to a slightly reduced control performance [4]. However, the aim of this paper is to provide a proof of concept, and not to provide a quantitative performance estimate. For this purpose the assumption of availability of a perfectly correlated reference signal seems to be justified.

Moreover, the static angle of attack is compensated in the reference signal to avoid the disturbance of proposed feed-forward control, e.g. by high-pass filtering. Note, that the alpha probe is generally used to measure the static angle of attack. For the adaptive MIMO feed-forward controller however only the alternating share of the alpha signal is used. The influence of pilot commands on the alpha probe measurement is also assumed to be compensated in the reference signal, in order to prevent the adaptive MIMO feed-forward controller from counteracting said pilot commands.

The elevator and symmetrically driven trailing edge flaps serve as actuators (i.e. the number of utilized actuators $M=2$.) Three different error sensors are considered. Two error sensors are dedicated to the compensation of unwanted atmospheric turbulence excited rigid body motions, namely the deviation of the pitch rate at the center of gravity q_{CG} from the pilot command $q_{CG_{pilot}}$, and the deviation of the vertical acceleration at the centre of gravity Nz_{CG} from the pilot command $Nz_{CG_{pilot}}$. For the compensation of atmospheric turbulence excited wing bending vibrations a modal wing bending sensor is defined as proposed in [1]:

$$Nz_{law} = \left[\frac{(Nz_{LW} + Nz_{RW})}{2} - Nz_{CG} \right] \quad (14)$$

Thereby Nz_{LW} and Nz_{RW} denote the vertical accelerations on the left and the right wing, and Nz_{CG} is the vertical acceleration at the centre of gravity. Finally the adaptive MIMO feed-forward control system can be illustrated as shown in Fig 1.

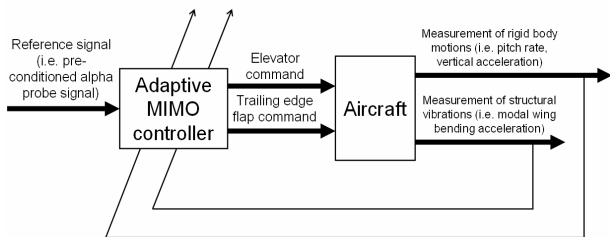


Fig. 1. The proposed adaptive MIMO feed-forward control system

In Fig 2. the transfer functions $G_{lm}(e^{j\omega T})$ of the transport aircraft model used in this paper are illustrated for one of the investigated wing tanks/Mach number configurations. In regards to controllability the symmetrically driven trailing edge flaps (TEFs) are appropriate for the compensation of Nz_{law} in the frequency range of structural modes (see dashed line with stars for $G_{Nz_{law},TEF}$), whereas the elevator (EL) naturally is mostly suitable for pitch control (see solid line for $G_{q_{CG},EL}$.) However the controllability Nz_{CG} is poor in the whole frequency range. Pitch control and control of wing bending vibrations is pretty much decoupled for this conventional configuration aircraft, which eases the adaptation of the FIR control filters \hat{h}_{mk} .

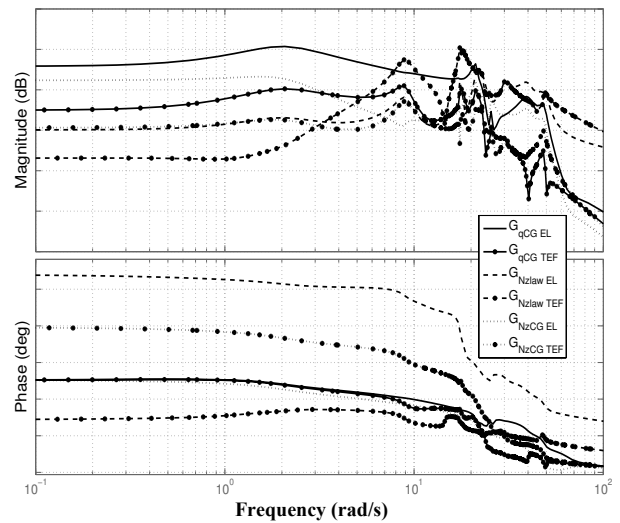


Fig. 2. Transfer functions $G_{lm}(e^{j\omega T})$ of the transport aircraft model

Three different control laws have been investigated:

- Control Law A: The $\Delta q_{CG} Nz_{law}$ control law
- Control Law B: The $\Delta Nz_{CG} Nz_{law}$ control law
- Control Law C: The $\Delta q_{CG} \Delta Nz_{CG} Nz_{law}$ control law

These three control laws are briefly discussed in the following:

A. The $\Delta q_{CG} Nz_{law}$ Control Law

The main objective of the proposed adaptive MIMO feed-forward control system is a simultaneous compensation of atmospheric turbulence excited pitch and wing bending. Thus, at first a control law aiming at the minimization of the quadratic H_2 norm of both, Nz_{law} , and the pitch rate

deviation Δq_{CG} is considered, with:

$$\Delta q_{CG} = q_{CG} - q_{CG_{pilot}} \quad (15)$$

Then the cost function J_A to be minimized is:

$$J_A = \langle \Delta q_{CG}^2 + Nz_{law}^2 \rangle \quad (16)$$

B. The $\Delta Nz_{CG} Nz_{law}$ Control Law

Since control law A increases vertical accelerations Nz_{CG} below 0.5 Hz, as Fig 3. shows, another control law is applied. This $\Delta Nz_{CG} Nz_{law}$ control law minimizes the deviation of the vertical acceleration at the centre of gravity from the pilot command ΔNz_{CG} instead of Δq_{CG} .

$$\Delta Nz_{CG} = Nz_{CG} - Nz_{CG_{pilot}} \quad (17)$$

Thus for control law B the cost function J_B is:

$$J_B = \langle \Delta Nz_{CG}^2 + Nz_{law}^2 \rangle \quad (18)$$

C. The $\Delta q_{CG} \Delta Nz_{CG} Nz_{law}$ Control Law

Since control law B leads to a poor pitch alleviation performance, and control law A even increases vertical accelerations Nz_{CG} below 0.5 Hz, a more complex control law aiming at the minimization of the quadratic H_2 norm of all 3 error signals is proposed. For such a control law the cost function makes:

$$J_C = \langle \Delta q_{CG}^2 + \Delta Nz_{CG}^2 + Nz_{law}^2 \rangle \quad (19)$$

D. Simulation Results

The numeric simulations start with zero-initialized controller $\bar{h}_{mk}(n=0)$, i.e.:

$$\bar{h}_{mk}(n=0) = [0, 0, \dots, 0]^T \text{ for } m=1,2 \text{ and for } k=K=1 \quad (20)$$

For convenience pilot inputs are neglected in the following:

$$q_{CG_{pilot}} = Nz_{CG_{pilot}} = 0 \quad (21)$$

The performance of the converged controller is measured after 10000 samples of adaptation to different wing

tanks/Mach number configurations. The plant models $\hat{G}_{lm}(f)$ used for the controller adaptation are perfect representations of $G_{lm}(f)$, so that $F_{error_{lm}}(f)=1$. The sampling time T of the controller is chosen to 40 ms. For the filter length $N=64$ showed to be a good compromise between high control performance and low computational costs. In Fig 3. the standardized magnitudes of the pitch rate q_{CG} , the vertical acceleration Nz_{CG} , and the modal wing bending acceleration Nz_{law} on the uncontrolled aircraft (solid lines) are compared with the according magnitudes with different control laws for one of the investigated wing tanks/Mach number configurations. The dashed lines illustrate the resulting magnitudes for the aircraft with control law A, whereas the dotted lines illustrate the resulting magnitudes for the aircraft with control law B. Finally, the dash dotted lines represent the corresponding magnitudes for the aircraft with control law C.

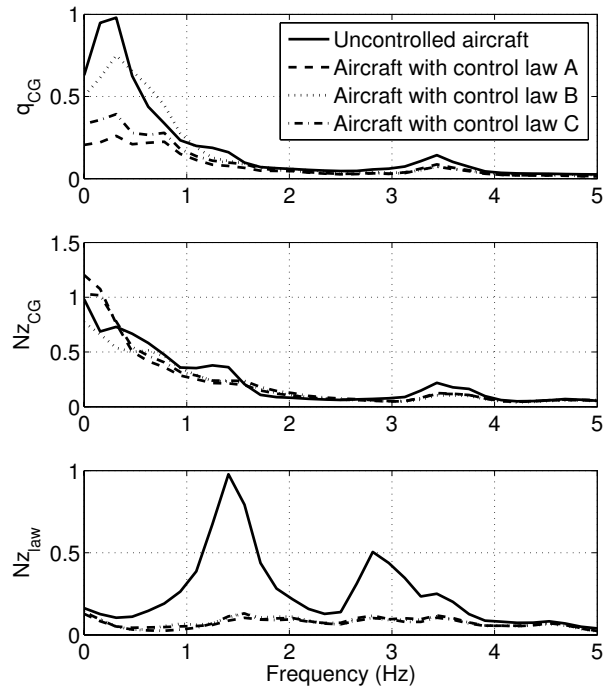


Fig. 3. Magnitudes of q_{CG} , Nz_{CG} , and Nz_{law} over frequency for different control laws with pre-conditioned reference signal.

It can be observed from Fig 3. that the potential for feed-forward compensation of modal wing bending accelerations Nz_{law} is very high as already argued in [5]. Also the atmospheric turbulence excited pitch rate q_{CG} can be well reduced with control law C, and even better with control law

A. The compensation of atmospheric turbulence excited vertical accelerations Nz_{CG} is poor for all control laws due to the low controllability of Nz_{CG} by the elevator, and the trailing edge flaps on the considered aircraft model. Moreover, vertical accelerations are even excited by control laws A and C. Control law C can at least limit the control excitation of vertical accelerations, but also shows reduced pitch compensation. If the aim is also a good Nz_{CG} compensation, introduction of direct lift control actuators (e.g. spoilers) would be required.

IV. CONCLUSION

In this paper an adaptive MIMO feed-forward controller is designed for simultaneous compensation of atmospheric turbulence excited rigid body motions and structural vibrations on a large conventional four-engine transport aircraft. An alpha probe is used as reference sensor, whereas the elevator and symmetrically driven trailing edge flaps serve as actuators.

At first, a control law for simultaneous minimization of the quadratic H_2 norms of atmospheric turbulence excited pitch rate and modal wing bending acceleration is applied. Unfortunately, this control law excites vertical accelerations in the frequency range of rigid body motions.

Thus, another control law for the simultaneous reduction of modal wing bending accelerations and vertical aircraft accelerations is applied to the aircraft model. This second control law slightly decreases unwanted vertical accelerations, but has a decreased performance on atmospheric turbulence excited pitch rate reduction.

Therefore, a more complex feed-forward control law is proposed that aims at the minimization of all three quantities, namely pitch rate, modal wing bending acceleration, and vertical acceleration, even though the additional introduction of direct lift control actuators (e.g. spoilers) would be more suitable for the reduction of atmospheric turbulence excited vertical accelerations.

Anyway, it could be shown that the proposed MIMO feed-forward controller with elevator and trailing edge flaps as actuators simultaneously compensates atmospheric turbulence excited pitch and wing bending to a high extend.

The advantage of adding the proposed adaptive MIMO feed-forward controller to conventional feedback gust load alleviation systems is an increased alleviation of atmospheric turbulence excited rigid body motions and structural vibrations. This results in better passenger comfort and handling qualities, as well as in reduced dynamic wing loads.

The adaptation increases the robustness of the performance of the feed-forward controller against modeling errors and variations of the wing tanks configuration and the Mach number. This is due to the potential adaptability of the

convergence coefficient to uncertainties in the plant model, compare (12). Using the proposed boundaries for the convergence coefficients, the convergence of the adaptation algorithm was always stable in the numeric simulations. However, a rigorous stability proof would still be required for the adaptive MIMO feed-forward control system before being implemented on a flying aircraft.

Pitch control and control of wing bending vibrations is pretty much decoupled on a conventional aircraft configuration which eases the control law design as well as controller adaptation. Moreover, the frequency range of rigid body motions is well separated from the frequency range of aeroelastic modes.

On *unconventional* future transport aircraft configurations however, MIMO feed-forward control law design for simultaneous compensation of atmospheric turbulence excited rigid body motions and structural vibrations is expected to be more difficult. Elasticity is expected to be increased on future configurations by the use of new weight efficient materials, making frequency separation between rigid and aeroelastic modes more difficult.

Moreover, on (fuel efficient) tailless aircraft, rigid body control and vibration control can be highly coupled. Such coupling increases the complexity of controller adaptation. Thus, subsequent research activities will be dedicated to multi-objective adaptive MIMO feed-forward control of plants with higher mode density, and with higher cross coupling between the actuators and the quantities that shall be minimized.

REFERENCES

- [1] M. Jeanneau, N. Aversa, S. Delannoy, and M. Hockenhull, "Awiator's study of a Wing Load Control: Design and Flight-test Results," *16th IFAC Symposium on Automatic Control in Aerospace*, St. Petersburg (RUSSIA), 14.-18. June, 2004.
- [2] A. Ayache, C. Ghiappa, and G. Puyou, "Gain Scheduling using Multimodel Eigenstructure Assignment: A new Application," *5th IFAC Symposium on Robust Control Design*, Toulouse, France, 05.-07. July, 2006.
- [3] R. König, K.-U. Hahn, and J. Winter, "Advanced Gust Management System," *Flight Mechanics Panel Symposium*, Turin, Italy, 09.-13. May, 1994.
- [4] A. Wildschek, R. Maier, R. Jategaonkar, and H. Baier, "Augmentation of active wing bending control with a supplementary adaptive feed-forward control algorithm," *EUCASS 2007 - 2nd European Conference For Aerospace Sciences*, Brussels, Belgium, 01.-06. July, 2007.
- [5] A. Wildschek, R. Maier, F. Hoffmann, M. Jeanneau, and H. Baier, "Active Wing Load Alleviation with an Adaptive Feed-forward Control Algorithm," *AIAA Guidance, Navigation, and Control Conference and Exhibit*, Keystone, CO, 21.-24. August, 2006.
- [6] S. Hecker, and K.-U. Hahn, "Advanced Gust Load Alleviation System for Large Flexible Aircraft," *1st CEAS European Air & Space Conference*, Berlin, Germany, 10.-13. September, 2007.
- [7] S. ELLIOTT, *Signal Processing for Active Control*, Academic Press, London, 2001, pp. 261.
- [8] G. Moschytz, and M. Hofbauer, *Adaptive Filter*, Springer, Berlin, 2000.
- [9] S. ELLIOTT, *Signal Processing for Active Control*, Academic Press, London, 2001, pp. 241-243.